Trans Indian Inst Met (2015) 68(6):1101–1106
DOI 10.1007/s12666-015-0653-2

TECHNICAL PAPER

Role of Ultrasonic Treatment on Microstructural Evolution in A356/TiB_2 In-Situ Composite

Jayakrishnan Nampoothiri[1] · Baldev Raj[1,2] · K. R. Ravi[1]

Received: 30 June 2015 / Accepted: 18 August 2015 / Published online: 11 September 2015

Abstract The present study explores the possibility of using ultrasonic treatment for the conversion of dendritic microstructure of in-situ A356/TiB_2 composite into non-dendritic globular structure. A356/2TiB_2 in-situ composite has been subjected to high intensity ultrasonic treatment in liquid metal state as well as during the process of solidification. Microstructural analysis shows that the ultrasonic treatment during the process of solidification is an effective technique for the transformation of dendritic morphology into fine globular structure along with the modification of Si needles.

Keywords Ultrasonic cavitation · Aluminum composites · Microstructure modification · Solidification · Non-dendritic structure

1 Introduction

Al–Si alloys are considered as promising materials for automobile and aerospace applications due to their castability, weldabiliy, and corrosion characteristics [1–3]. In recent time, there is a significant interest towards particulate reinforced composites made from these alloys because of their high Strength-to-Weight ratio [4]. However, dendritic microstructure, non-uniform distribution of reinforcement particles and coarse second phase particles reduces their mechanical properties, more specifically the fracture toughness and ductility of aluminum matrix composites, which restrict their wider usage [5].

The commonly used methods for getting a non-dendritic microstructure by solidification controlling are (a) Mechanical Stirring, (b) Magneto hydrodynamic stirring, (c) Chemical grain refinement, and (d) cooling slope method etc. [6]. Even though Mechanical Stirring and Cooling Slope methods are cost effective, oxidation, gas entrapment and stirrer dissolution impedes its commercialization [6–8]. Moreover, mechanical stirring is able to produce only rosette type of structure rather than a spherical one. Magneto Hydrodynamic stirring is a non-contact agitating method where electromagnetic induction stirring effect is utilized [9]. In this method, combinations of multiple coils are required to get a uniform microstructure. Electromagnetic coils consumes huge amount of energy and thus it reduces its cost effectiveness. Chemical refinement is a non-agitating route where inoculant particle are added to enhance nucleation. Though it is a cost effective and contamination free method, it is restricted to limited numbers of alloy systems [10]. Ultrasonic treatment (UT) can be considered as an alternative approach to overcome aforementioned drawbacks since it is applicable for mass production and cost effective. In addition to that the degassing ability of UT makes an interesting choice for non-dendritic microstructure development.

In recent years, employment of ultrasonic treatment in metallurgical application has been studied extensively. It has been accepted that the injection of high energy ultrasonic waves to liquid media give rise to non-linear effects which can reduce the particle size, modify the dendritic structure, refine the equi-axed grains and improves the dispersion of particles [11–14]. Recently, Wang et al. [15] studied the effect of ultrasonic treatment

✉ K. R. Ravi
krravi.psgias@gmail.com

[1] Structural Nanomaterials Laboratory, PSG Institute of Advanced Studies, Coimbatore, Tamil Nadu 641 004, India

[2] National Institute of Advanced Studies, Bangalore, Karnataka 560 012, India

in refining grain structure during solidification of Al-Cu alloy and observed a transition from dendritic to equi-axed structure along with 10 fold refinement in grain size. Kotadia et al. [16] reported the modification of hypo and hyper-eutectic Al–Si alloys under ultrasonic irradiation. They also found that it is an effective tool to obtain non-dendritic equi-axed microstructure. Even though UT has a great potential towards grain refining, microstructure modification etc., there is not much work reported on effect of UT on microstructural evolution of in-situ aluminum composites. Inspired by the previous work on unreinforced alloy systems, the role of ultrasonic treatment on microstructural evolution of A356/2TiB_2 in-situ composites has been investigated in the present work.

2 Experimental Details

A356-2wt% TiB_2 composite was prepared by adding pre-heated mixture of K_2TiF_6 and KBF_4 salts in the required stoichiometric ratio to the A356 Al alloy melt at 800 °C. The melt was stirred at a regular interval of 10 min to enhance mixing and thus the exothermic reaction to form TiB_2 particles. After the one hour reaction, the slag and dross formed on the melt surface were completely removed and thereafter 0.3 wt% of pure magnesium was added to compensate the Mg loss [17]. Subsequently, the composite melt was transferred to a pre-heated (750 °C) stainless steel mould of height 6 cm and diameter 5 cm to perform ultrasonic treatment. A magnetorestrictive transducer with SS304 horn (RELTEC, Russia) operated at a power output of 2 kW was used to perform UT experiments.

Ultrasonic treatment was carried out by introducing the pre-heated (750 °C) sonotrode into the stainless steel mould. Ultrasonic treatment was conducted in two different temperature ranges (i) UT in liquid melt, named as liquid melt treatment (LMT) (ii) UT during solidification, referred as solidification melt treatment (SMT). The LMT was performed in the liquid melt for 120 s by maintaining the melt temperature isothermally at 750 °C. SMT started in liquid state at a melt temperature of 750 °C and continued till the melt temperature reaches 567 °C. The choice of temperatures used for SMT study is explained in the succeeding section with the help of Scheil solidification curve (Fig. 1). During UT, depth of immersion of sonotrode below the melt surface was maintained as 5 mm. After ultrasonic treatment the melt was allowed to cool in the mould itself. The samples were cut, ground and polished prior to electrolytic etching using 2 % HBF_4 solution. The microstructural analysis was carried out using Carl Zeiss Axio Scope A1 polarized light microscope and the morphology of Si needle was analyzed using FESEM (Carl Zeiss, Sigma, UK). The reinforcement particles were

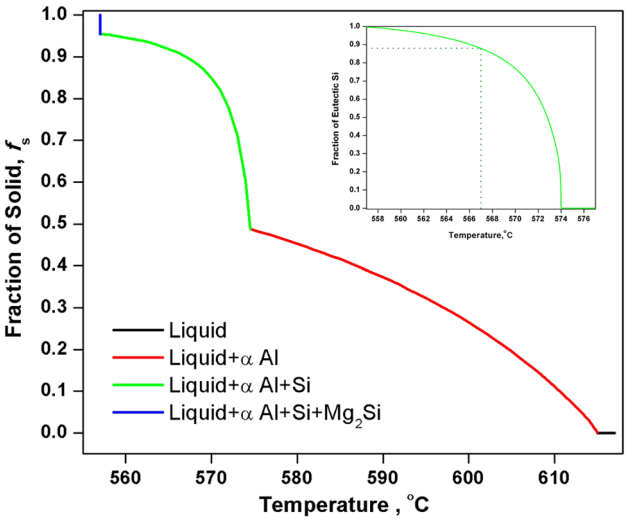

Fig. 1 Temperature versus liquid fraction curve of A356 aluminum alloy

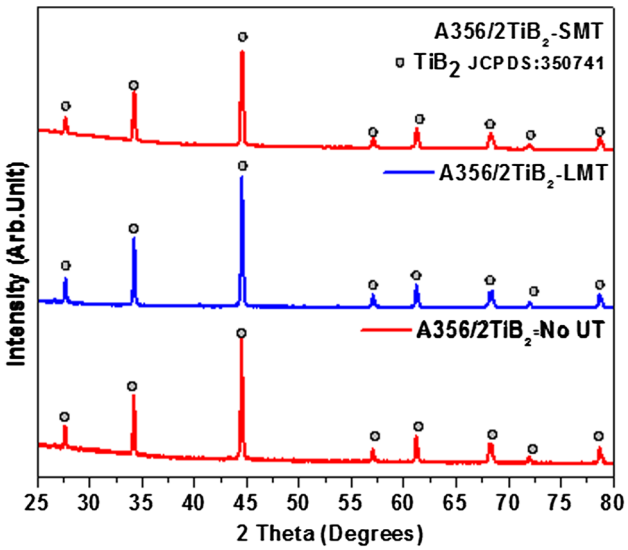

Fig. 2 XRD pattern of particles extracted from the A356/2TiB_2 composite without and with UT

extracted from the composites by dissolving the matrix in NaOH solution and the extracted particles were analyzed using the X-ray diffraction method with Cu-K_α radiation (Shimadzu XD-D1).

3 Results and Discussion

The X-Ray diffractogram of powders extracted from both treated and untreated composites are provided in Fig. 2. XRD pattern of particles extracted from untreated A356/2TiB_2 composite closely matches with the standard pattern of TiB_2 particles (JCPDS: 350741). It confirms the

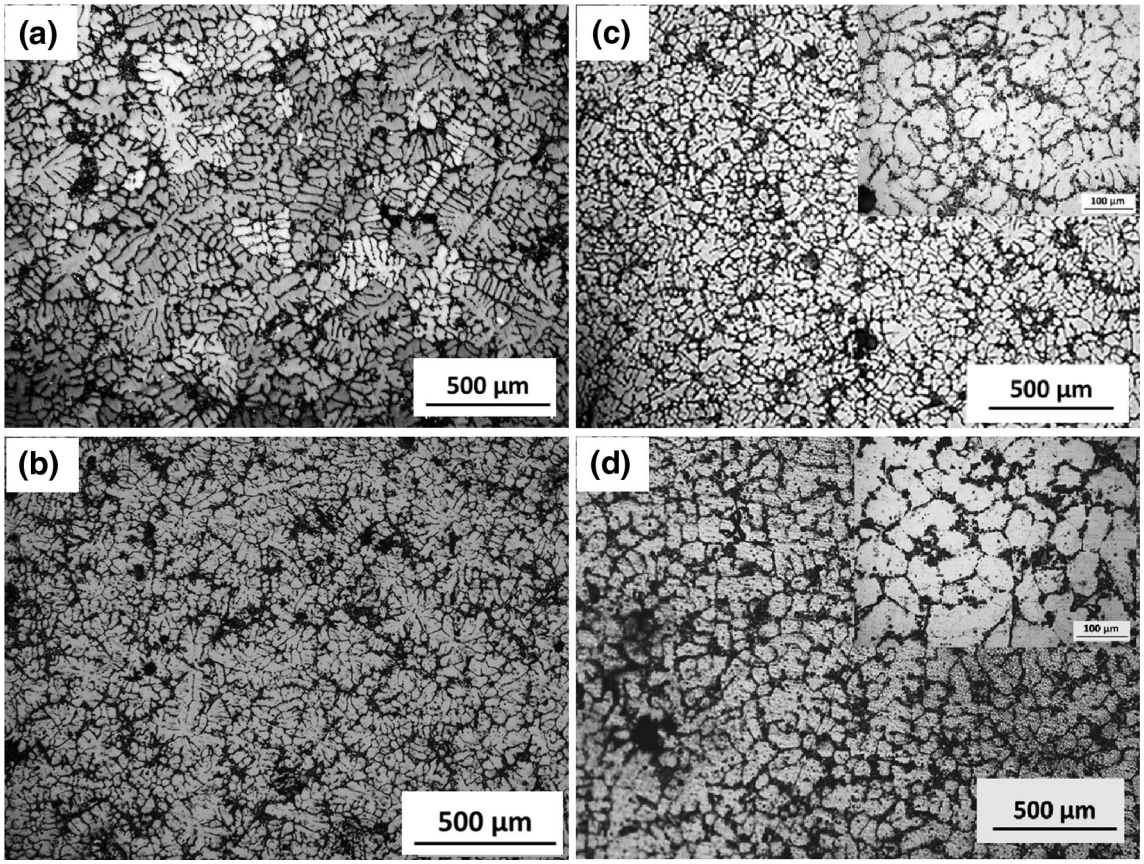

Fig. 3 Optical Micrograph of **a** A356 alloy, A356/2TiB_2 composite **b** as cast, **c** with LMT, **d** with SMT

formation of TiB_2 particles via in situ reactions and it also suggests the nonexistence of other brittle intermetallic phases like Al_3Ti within the XRD detection limit. Close resemblance of XRD profiles and absence of any other phases in XRD diffractogram of particles extracted from untreated, LMT and SMT A356 Al/2TiB_2 composites reaffirms that the TiB_2 particles are stable during ultrasonic treatment.

The influence of ultrasonic treatment on microstructure modification in A356/2TiB_2 composites is illustrated in Fig. 3. Figure 3a represents the as cast microstructure of A356 aluminum alloy, which exhibits an archetypal dendritic microstructure. The primary α-Al dendrite in the alloy appears elongated with high aspect ratio of 3.75. Figure 3b shows the microstructure of A356/2TiB_2 composite without ultrasonic treatment. Similar to A356 alloy, microstructure of A356/2TiB_2 composites comprises dendritic morphology. However the dendrite arm lengths of composites are shorter than that of alloy and the average aspect ratio of dendritic structure in as cast composite is obtained as 1.78. It implies that that the presence of TiB_2 particle plays a critical role in reducing the dendritic arm length. Fan et al. [18] has analyzed the crystallographic match between TiB_2 particle and aluminum alloy. They found that the TiB_2 and α-Al have low planar mismatch in some close packed planes and hence proposed TiB_2 as a possible heterogeneous nucleation site for α-Al. Nevertheless all the particles present in the melt will not instigate nucleation, only the particles which are active in the given melt condition can cause the nucleation. The microstructural analysis of A356/2TiB_2 composites exhibits a dendritic structure, which indicates that the sufficient active nucleant particles are not available for the formation of globular structure. Moreover, the analysis of micrograph gives an insight that the major fractions of TiB_2 particles are situated at grain boundary and interdendritic region. It suggests that during solidification, TiB_2 particles are pushed towards the solid–liquid interface; which can effectively control the growth of dendrites. Hence, dendritic arm length of A356/2TiB_2 composites got reduced due to the synergistic effect of heterogeneous nucleation and the dendritic arm growth restriction induced by TiB_2 particles.

Figure 3c, d represent the microstructure of A356/2TiB_2 composites after subjecting to ultrasonic treatment. When the ultrasonic treatment is performed in LMT mode (Fig. 3c), the microstructure of A356 Al/TiB_2 composite is converted into rosette-like grain structure with marginal

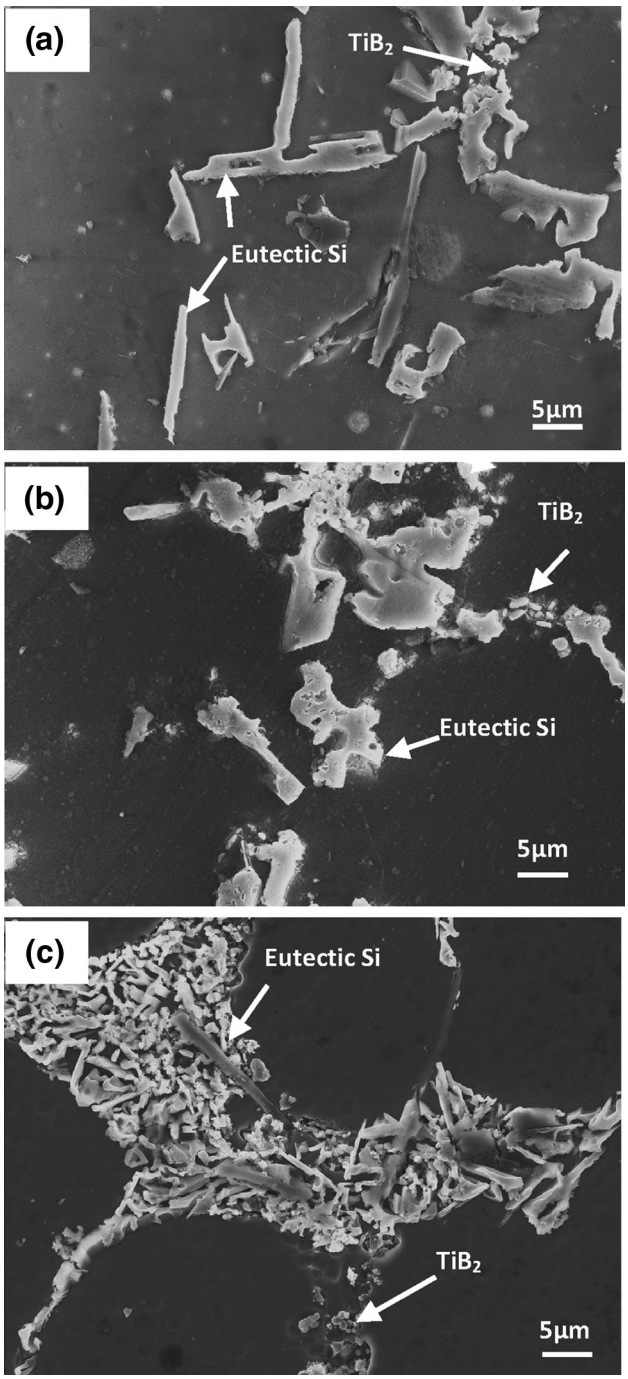

Fig. 4 FESEM image of A356/TiB_2 **a** as cast composites, composites subjected to **b** LMT **c** SMT

reduction in the average aspect ratio into 1.41. The mechanism of grain structure modification during LMT can be discussed with the non-linear effect of ultrasound in liquids namely, acoustic cavitation. During UT, liquid molecule compresses and expands on the positive and negative half cycle, respectively. When acoustic pressure exceeds a value characteristic to a particular liquid [19], bonding between the liquid molecules break. It results in the formation of numerous tiny cavities which upon pulsation, rapidly grows by the inward diffusion of gases in the melt and finally they implode. During the cavitation implosion, extremely high temperature, pressure and powerful shock waves are generated in the localized region [20]. According to Clausius–Clayperon equation, the pressure increment instigated by cavitation implosion produce localized undercooling effect on melt [21]. Potency of nucleant particles such as TiB_2 get further improved in the presence of local undercooling. In addition to this, shock waves generated during cavitation implosion cleans the surface of TiB_2 particles and thereby enhances the wetting of TiB_2 particles with molten Al. Consequently, LMT improves the nucleation potency of TiB_2 particles and thereby changes the morphology of grain structure.

The temperature versus liquid fraction curve of A356 Al alloy is calculated based on Scheil solidification simulation to determine the start and end temperature for SMT. According to Fig. 1, the solidification of α-Al starts at 614 °C and the entire solidification process completes at 554 °C. Based on solidification simulation curve, SMT treatment is carried out up to 567 °C, i.e. up to 0.8 fraction of solid. Ultrasonic wave transfer beyond this fraction of solid is extremely difficult because the entire melt becomes mushy [22]. Figure 3d shows the microstructure of A356 Al/TiB_2 composite treated with ultrasound during solidification. It can be seen that the SMT converts dendritic microstructure into nearly globular structure. Similar to aspect ratio calculation in dendritic microstructures, non-dendritic globular microstructures are quantified by the term "Sphericity factor (S_F)" using the following equation [23]:

$$S_F = \frac{4\pi A}{L_P^2} \tag{1}$$

where, A is the sectional area of individual globular structure, L_p is the circumference of respective globules. The value of S_F varies from 0 to 1, and when it is closer to 1, the cross-sectional shape of globules becomes perfect circular in morphology. In the present study, the sphericity factor of SMT A356/2TiB_2 composite is found to be 0.794 ± 0.085. It indicates that the ultrasonic treatment during solidification is effective in converting dendritic microstructures into globular kind. Ultrasonic cavitation implosion during solidification plays a critical role in the formation of globular microstructure along with the nucleation control. As in LMT, here also ultrasonically activated TiB_2 particle contributes to the formation of rosette-like structure. Powerful shock waves formed during cavitation implosion induces a strong stirring effect on the melt which advect hot and solute rich liquid metal towards the interface of dendritic crystals formed in preceding course of solidification. The localized temperature and

solute concentration variation at the dendritic interface re-melts the root of crystals and the shock waves carry the fragmented crystals, either to sub-cooled region or to super-heated zone in the melt [24]. The fragmented particles in sub-cooled region enhances further nucleation to form globular structure while the particles which are carried to hot zone may undergo dissolution. Moreover the shock wave assisted convection current can homogenize the melt to get a uniform structure [25]. Hence, the combined effect of activation of TiB_2 nucleant particle and dendrite fragmentation of UT leads to the formation the globular structure.

FESEM micrograph of A356/2TiB_2 composites represents the morphological evolution of eutectic Si needle during ultrasonic treatment (Fig. 4). Coarse acicular eutectic silicon is observed along TiB_2 particles in the interdendritic region of untreated A356 Al/TiB_2 composites (Fig. 4a). Figure 4b represents the microstructure of composite subjected to ultrasonic treatment in liquid stage, in which no noticeable change in the morphology of eutectic Si is observed. On the other hand, when UT of composite is carried out during solidification, very fine eutectic silicon of polygonal morphology is observed. The Si particles are as fine as the chemically modified one (Fig. 4c). Under normal solidification condition, the solute atoms usually segregate in front of the solid–liquid boundary which results in the formation of lengthy eutectic Si needles [26]. The solidification curve depicted in (inset) Fig. 1 points that eutectic Si formation starts at 574 °C and it ends by 557 °C. It is clear that the major fraction of eutectic Si (up to 0.9) is formed in the presence of UT. When UT is performed during solidification, the convection current generated by UT homogenizes the melt and thereby reduces the solute segregation in solidification front which effectively contributes in eutectic Si modification. Moreover, the cavitation implosion breaks the eutectic Si needle when shear force created by the shock wave exceeds the cracking strength of Si needles [27]. Microstructure investigation also reveals that a small fraction of the larger Si particles still exists. Based on scheil-solidifcation curve, it can be inferred that the UT is not continued till the complete formation of eutectic Si which allows the formation of lengthy eutectic Si needle under normal solidification condition. Further investigations are required to understand the exact mechanisms of Si modification under ultrasonic cavitation.

4 Summary

A356/2TiB_2 in-situ composite has been subjected to ultrasonic treatment (UT) in liquid metal as well as during solidification. An isothermal ultrasonic treatment of A356/2TiB_2 in-situ composite in liquid state reduces its aspect ratio of dendritic structure considerably, but this technique fails to produce a non-dendritic microstructure. A356/2TiB_2 composites with globular non-dendritic microstructure are obtained when subjected to ultrasonic treatment during solidification. Ultrasonic treatment of A356/2TiB_2 in-situ composite in liquid state has shown a marginal refinement in eutectic Si size. On the other hand, ultrasonic treatment during solidification modifies the acicular plate type eutectic Si morphology into compact-polygonal type and the average size of eutectic Si particle reduces from 28 to 3.4 μm. The non-linear effect of UT like cavitation implosion and the cavitation induced convection are considered as the major reasons for the significant microstructural modifications.

Acknowledgments The research work reported here was funded by the Directorate of Naval Research Board (NRB), Govt. of India. Grant Number: DNRD/05/4003/NRB/292. The authors were grateful to the support provided by NRB, India.

References

1. Murty B S, Maiti R, and Chakraborty M, *J Metall Mater Sci* **43** (2001) 93.
2. Kumar S, Chakraborty M, Sarma V S, and Murty B S, *Wear* **265** (2008) 134.
3. Li P, Kandalova E G, and Nikitin V I, *Mater Lett* **59** (2005) 2545.
4. Pramod S L, Bakshi S R, and Murty B S, *J Mater Eng Perform* **24** (2015) 2185.
5. Wang M, Chen D, Chen Z, Wu Y, Wang F, Ma N, and Wang H, *Mater Sci Eng A* **590** (2014) 246.
6. Mohammed M N, Omar M S, Salleh M S, Alhawari K S, and Kapranos P, *Sci World J.* doi:10.1155/2013/752175.
7. Flemings M C, *Metall Mater Trans A* **22** (1991) 957.
8. Haga T and Suzuki S, *J Mater Process Technol* **157–158** (2004) 695.
9. Zoqui E J, Paes M, and Es-Sadiqi E, *J Mater Process Technol* **120** (2002) 365.
10. Fan Z, *Int Mater Rev* **47** (2002) 49.
11. Li J, Momono T, Tayu Y, and Fu Y, *Mater Lett* **62** (2008) 4152.
12. Harini R S, Jayakrishnan N, Nagasivamuni B, Baldev R, and Ravi K R, *Mater Lett* **145** (2015) 328.
13. Roshini C P, Nagasivamuni B, Baldev R, and Ravi K R, *J Mater Eng Perform* **24** (2015) 2234.
14. Poovazhagan L, Kalaichelvan K, and Rajadurai A, *Trans IIM* **67** (2014) 229.
15. Wang G, Dargusch M S, Qian M, Eskin D G, and StJohn D H, *J Cryst Growth* **408** (2014) 119.
16. Kotadia H R, and Das A, *J Alloys Compd* **620** (2015) 1.
17. Mandal A, Chakraborty M, and Murty B S, *Mater Sci Eng A* **489** (2008) 220.
18. Fan Z, Wang Y, Zhang Y, Qin T, Zhou X R, Thompson G E, Pennycook T, and Hashimoto T, *Acta Mater* **84** (2015) 292.
19. Eskin G I, *Ultrason Sonochem* **8** (2001) 319.
20. McNamara W B III, Didenko Y T, and Suslick K S, *Nature* **401** (1999) 772.
21. Atamanenko T V, Eskin D G, Zhang L, and Katgerman L, *Metall Mater Trans A* **41A** (2010) 2056.
22. Zhang L, Eskin D G, Miroux A, and Katgerman L, *Light Metals 2012 TMS* (2012) 999.

23. Aghayani M K, and Niroumand B, *J Alloys Compd* **509** (2011) 114.
24. Jian X, Xu H, Meek T T, and Han Q, *Mater Lett* **59** (2005) 190.
25. Liu Q, Zhang Y, Song Y, Qi F, and Zhai Q, *Mater Des* **28** (2007) 1949.
26. McDonald S D, Nogita K, and Dahle A K, *Acta Mater* **52** (2004) 4273.
27. Puga H, Barbosa J, Costa S, Ribeiro S, Pinto A M P, and Prokic M, *Mater Sci Eng A* **560** (2013) 589.